FEBS Letters 586 (2012) 1141–1146

FEBS Letters

journal homepage: www.FEBSLetters.org

NMR characterization of the interaction between the PUB domain of peptide:*N*-glycanase and ubiquitin-like domain of HR23

Yukiko Kamiya [a,b], Yoshinori Uekusa [a,b], Akira Sumiyoshi [b], Hiroaki Sasakawa [b,c], Takeshi Hirao [b], Tadashi Suzuki [d], Koichi Kato [a,b,c,e,f,*]

[a] *Okazaki Institute for Integrative Bioscience, National Institutes of Natural Sciences, 5-1 Higashiyama, Myodaiji, Okazaki, Aichi 444-8787, Japan*
[b] *Graduate School of Pharmaceutical Sciences, Nagoya City University, 3-1 Tanabe-dori, Mizuho-ku, Nagoya 467-8603, Japan*
[c] *Institute for Molecular Science, National Institutes of Natural Sciences, 5-1 Higashiyama, Myodaiji, Okazaki, Aichi 444-8787, Japan*
[d] *Glycometabolome Team, Systems Glycobiology Research Group, RIKEN Advanced Science Institute, 2-1 Hirosawa, Wako, Saitama 351-0198, Japan*
[e] *The Glycoscience Institute, Ochanomizu University, 2-1-1 Ohtsuka, Bunkyo-ku, Tokyo 112-8610, Japan*
[f] *GLYENCE Co., Ltd., 2-22-8 Chikusa, Chikusa-ku, Nagoya 464-0858, Japan*

ARTICLE INFO

Article history:
Received 25 February 2012
Accepted 9 March 2012
Available online 23 March 2012

Edited by Christian Griesinger

Keywords:
PUB domain
Peptide:*N*-glycanase
HR23
NMR
Endoplasmic reticulum-associated degradation
Ubiquitin–proteasome system

ABSTRACT

PUB domains are identified in several proteins functioning in the ubiquitin (Ub)–proteasome system and considered as p97-binding modules. To address the further functional roles of these domains, we herein characterized the interactions of the PUB domain of peptide:*N*-glycanase (PNGase) with Ub and Ub-like domain (UBL) of the proteasome shuttle factor HR23. NMR data indicated that PNGase-PUB exerts an acceptor preferentially for HR23–UBL, electrostatically interacting with the UBL surface employed for binding to other Ub/UBL motifs. Our findings imply that PNGase-PUB serves not only as p97-binding module but also as a possible activator of HR23 in endoplasmic reticulum-associated degradation mechanisms.

Structured summary of protein interactions:
PNGase binds to **HR23A** by affinity chromatography technology (View interaction)
PNGase and **HR23A** bind by nuclear magnetic resonance (View interaction)
PNGase and **HR23B** bind by nuclear magnetic resonance (View interaction)

1. Introduction

Ubiquitin (Ub)–proteasome-mediated proteolysis plays a crucial role in a number of diverse processes in eukaryotic cells by controlling the levels of intracellular regulatory proteins and by eliminating potentially toxic malfolded proteins [1–4]. In the early secretory pathway, glycoproteins are subjected to the quality control mechanisms depending on the Ub–proteasome pathway. In this system, high-mannose-type *N*-glycans that modify proteins serve as *quality tags* that are recognized by intracellular lectins operating as molecular chaperones and cargo receptors in the endoplasmic reticulum (ER) [5–7]. Secretory glycoproteins that eventually fail to acquire their correct conformations are recognized by ER luminal lectins, such as OS-9, and are retrotranslocated through a multi-protein retrotranslocation channel to the cytosol, wherein they are degraded by the Ub–proteasome pathway. Accumulating evidence indicates that the proteins involved in ER-associated degradation (ERAD) machinery form a huge membrane-spanning complex [8–10]. The cytosolic components of the ERAD machinery include the AAA ATPase complex p97 and peptide:*N*-glycanase (PNGase) [11,12].

The ERAD substrates are retrotranslocated from the ER to the cytosol by the action of p97 ATPase and undergo ubiquitination and deglycosylation [13–15]. The deglycosylation enzyme PNGase facilitates ERAD by cleaving the bulky *N*-glycans from the substrates prior to their proteasomal degradation [16,17]. This enzyme recruits the proteasome shuttle factor HR23, which consists of an N-terminal Ub-like domain (UBL), two Ub-associated (UBA) domains, and a xeroderma pigmentosum group C binding (XPCB) domain [11,18,19]. In mammals, cytosolic PNGase comprises a central catalytic domain and flanking N- and C-terminal domains, which are not conserved in yeast PNGase [20]. The N-terminal domain of PNGase is tethered to p97, while the C-terminal domain has lectin activity that is specific for larger high-mannose-type oligosaccharides [7,21].

The N-terminal domain of PNGase is termed PUB for "PNGase/UBA or UBX" because its homologous domains have been identified

* Corresponding author at: Okazaki Institute for Integrative Bioscience, National Institutes of Natural Sciences, 5-1 Higashiyama, Myodaiji, Okazaki, Aichi 444-8787, Japan. Fax: +81 564 59 5224.
E-mail address: kkatonmr@ims.ac.jp (K. Kato).

0014-5793/$36.00
http://dx.doi.org/10.1016/j.febslet.2012.03.027

in proteins containing the UBA or ubiquitin regulatory X (UBX) domain, which also provides a p97-interacting motif [22–26]. For example, the p97-interacting protein Ubxd-1 contains PUB and UBX, while the HOIL-1L interacting protein (HOIP) possesses PUB and UBA domains [26]. Because the UBA and UBX domains are often found in proteins involved in the Ub–proteasome system, the PUB domains are supposed to be functionally linked to the intracellular protein degradation system [22,26]. However, although PUB has been reported to act as a p97 regulator through an interaction with its C-terminal segment in a phosphorylation-dependent manner, the functional roles of PUB remain largely unknown [27–29].

Besides p97, the PUB domain of mouse PNGase has been shown, by yeast two-hybrid experiments, to interact with a variety of proteins involved in ERAD, i.e. ERAD E3 enzyme gp78, putative member of retrotranslocon pore Derlin-1, proteasome subunit S4, and Ub as well as HR23 [11,20]. Although a crystallographic study revealed that the XPCB domain of HR23 binds the catalytic domain of PNGase [19], an in vitro pull-down assay indicated that PUB is capable of interacting directly with HR23–UBL [30,31]. To gain further insight into the functional role of PNGase–PUB in the ERAD machinery, the interactions of PNGase–PUB with UBLs and Ub chains were analyzed in a quantitative manner by frontal affinity chromatography (FAC) and NMR spectroscopy.

2. Materials and methods

2.1. Protein expression and purification

Human Ub, Ub E1, and E2-25K were expressed and purified, as described previously [32]. The DNA fragment for residues 1–117 which correspond to the mouse PNGase–PUB domain (Supplementary Fig. 1) was cloned into the BamHI and XhoI sites of the pGEX-6p1 vector (GE Life Science). The coding sequences of the UBL domains of human HR23a and HR23b (Supplementary Fig. 1) were inserted into the pGEX-6t1 vector using NotI and BamHI sites. Each protein was expressed in *Escherichia coli* BL21(DE3) CodonPlus and purified with a glutathione–sepharose column (GE Life Science) that was equilibrated with 50 mM Tris–HCl (pH 8.0) containing 0.1 M NaCl. The cells were grown in M9 minimal media containing [^{15}N]NH_4Cl (1 g l^{-1}) and/or [U-$^{13}C_6$]glucose to produce isotopically labeled proteins, according to the protocol described previously [33]. Lys48-linked Ub chains were prepared by an in vitro enzymatic reaction using E1 and E2-25K, as described previously [32,34].

2.2. NMR measurement

All NMR samples were dissolved in 10 mM sodium phosphate buffer (pH 7.0) containing 10% ^2H_2O (v/v) and 0.01% NaN_3. Spectral data were recorded at 303 K using a JEOL ECA-600 spectrometer or Bruker DMX500 spectrometer equipped with 5-mm inverse triple-resonance probes with three-axis gradient coils. Spectral assignments of PNGase–PUB were made by 2D ^{1}H–^{15}N HSQC, 3D CBCA(CO)NH, and 3D CBCANH experiments at 303 K. Although the spectral assignment of HR23b–UBL was reported previously [35], the data were collected at a different buffer condition than that used in the present study. Therefore, we assigned the backbone resonance of HR23b–UBL by the triple resonance experiments. Chemical shift perturbations (CSPs) observed for ^{15}N-labeled protein (0.3 mM) titrated with 0.3–1.5 mM concentration of non-labeled titrant were quantified as $\Delta\delta = [(\Delta\delta_H)^2 + (\Delta\delta_N/5)^2]^{1/2}$, where $\Delta\delta_H$ and $\Delta\delta_N$ are the observed chemical shift changes for ^{1}H and ^{15}N, respectively. The dissociation constant K_d (=1/K_a) was determined by fitting the observed CSPs in the protein signals in the course of titration to a single-binding site model (P + L ⇄ PL) using the following equations [36]:

$$\Delta\delta_{\text{observed}} = \Delta\delta_{\text{bound}} \times \theta;$$

$$\theta = \frac{[PL]}{[P_t]} = \frac{([P_t] + [L_t] + K_d) - \sqrt{([P_t] + [L_t] + K_d)^2 - 4[P_t] \times [L_t]}}{2[P_t]} \quad (1)$$

Here, $\Delta\delta_{\text{bound}}$ indicates the CSP value in a fully bound state (i.e., at saturation), and θ is the fractional population of the bound state at a given titration point, characterized by the total molar concentrations of the protein ($[P_t]$) and ligand ($[L_t]$) in the sample. The data were processed using NMRPipe [37] and analyzed using Sparky [38].

2.3. FAC analyses

FAC analyses were performed according to the literature [39–41] with modifications. PNGase–PUB was coupled to a HiTrap NHS-activated column (GE Healthcare) according to the manufacturer's instructions. After immobilization, the agarose beads were removed from the cartridge and packed into a stainless steel column (4.0 × 10 mm) (GL Sciences). Protein analytes, including HR23a–UBL, Ub, and Ub chains, were dissolved at 20 μM in 10 mM sodium phosphate buffer (pH 7.0) and applied to the PNGase–PUB column at a flow rate of 0.25 ml min^{-1}. The elution profiles were monitored by UV absorption at 230 nm. The binding affinity of each protein was calculated based on the retardation V_f–V_0 measured at a concentration of 20 μM using Eq. (2):

$$[A]_0(V_f - V_0) = B_t - \frac{1}{K_a(V_f - V_0)} \quad (2)$$

where $[A]_0$, V_0, and B_t are the concentration of UBL or Ub (chain), elution volume of the control protein, and total amount of immobilized PUB in the column, respectively. B_t was calculated from the K_a of HR23a–UBL, and Ub was obtained from the NMR CSP analyses. To determine V_0, myoglobin was used as a control protein for the analyses of PNGase–PUB. The retardation of each protein compared with that of myoglobin was computed using the difference of each elution volume, V_f.

2.4. Docking model

For 3D-structural model building, PNGase–PUB and HR23b–UBL were docked to one another by the HADDOCK program using the standard protocol based on the CSP data [42]. The computational structures of the complex between PNGase–PUB and HR23b–UBL were generated with HADDOCK2.1 [42,43] in combination with

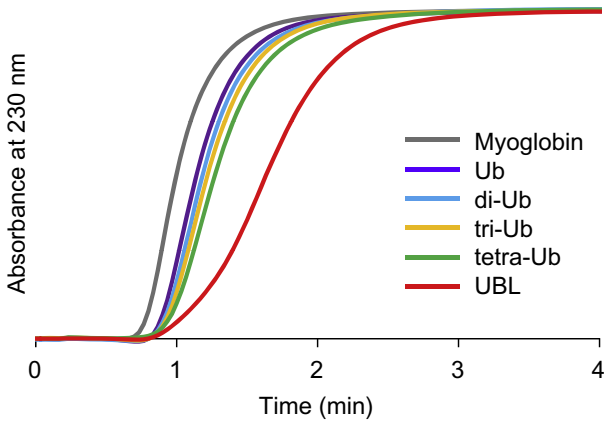

Fig. 1. Elution profiles of HR23a–UBL, Ub, and Ub chains after application to an immobilized PUB column. The elution profiles are superimposed on that of myoglobin.

Table 1
Association constants of PNGase–PUB for HR23–UBLs and Ub chains.

K_a, ($\times 10^3$ M^{-1})					
HR23a–UBL	HR23b–UBL	Ub	Di-Ub	Tri-Ub	Tetra-Ub
4.5[a]	4.8[a]	1.2[a]	1.5	1.7	2.2

[a] Determined from NMR titration data.

CNS [44]. The starting structures employed were based on the NMR structure of HR23 (PDB code: 1P1A) [35] and crystal structure of PNGase–PUB complexed with the terminal peptide of p97 (PDB code: 2HPL) [27]. In the latter structure, the atomic coordinates of the p97 peptide were removed prior to the calculation. For the rigid-body energy minimization, 1000 complexed structures were generated, initially based on the identified interaction surfaces.

3. Results

3.1. PNGase–PUB interacts with HR23–UBL and Ub chains

First, we performed FAC analyses to examine the relative affinities of the direct interactions of PNGase–PUB with Ub chains and the UBL domain of HR23a. Lys48-linked di-, tri-, and tetra-Ub chains were prepared by in vitro enzymatic reactions. Fig. 1 shows the overlaid elution profiles of the varying lengths of Ub chains along with that of HR23a–UBL, which were applied to the PUB-immobilized column. The elution retardations of UBL and Ub chains were observed and compared with that of the control protein myoglobin. These data indicate that PNGase–PUB binds to longer Ub chains with higher affinities and to HR23a–UBL with the highest affinity.

3.2. Binding affinities of PNGase–PUB for HR23–UBLs and Ub chains

We performed NMR titration analyses between PNGase–PUB and HR23a–UBL, HR23b–UBL, and Ub to determine the association constant (K_a) values of their interactions in a quantitative manner. As exemplified by the progressive chemical shift change of the ^1H–^{15}N HSQC peaks of PUB titrated with UBL or Ub (Supplementary Fig. 2), each interaction underwent a first-exchange regime. Hence, according to Eq. (1), we calculated the values of K_a as 4.5×10^3 M^{-1} for HR23a–UBL, 4.8×10^3 M^{-1} for HR23b–UBL, and 1.2×10^3 M^{-1} for Ub. With the K_a values of UBL and monomeric Ub thus determined from NMR titration data, the K_a values of each length of Ub chain were calculated on the basis of the relative affinities estimated from the elution volume $V_f - V_0$ in the FAC analyses according to Eq. (2) (Table 1). The results demonstrated that

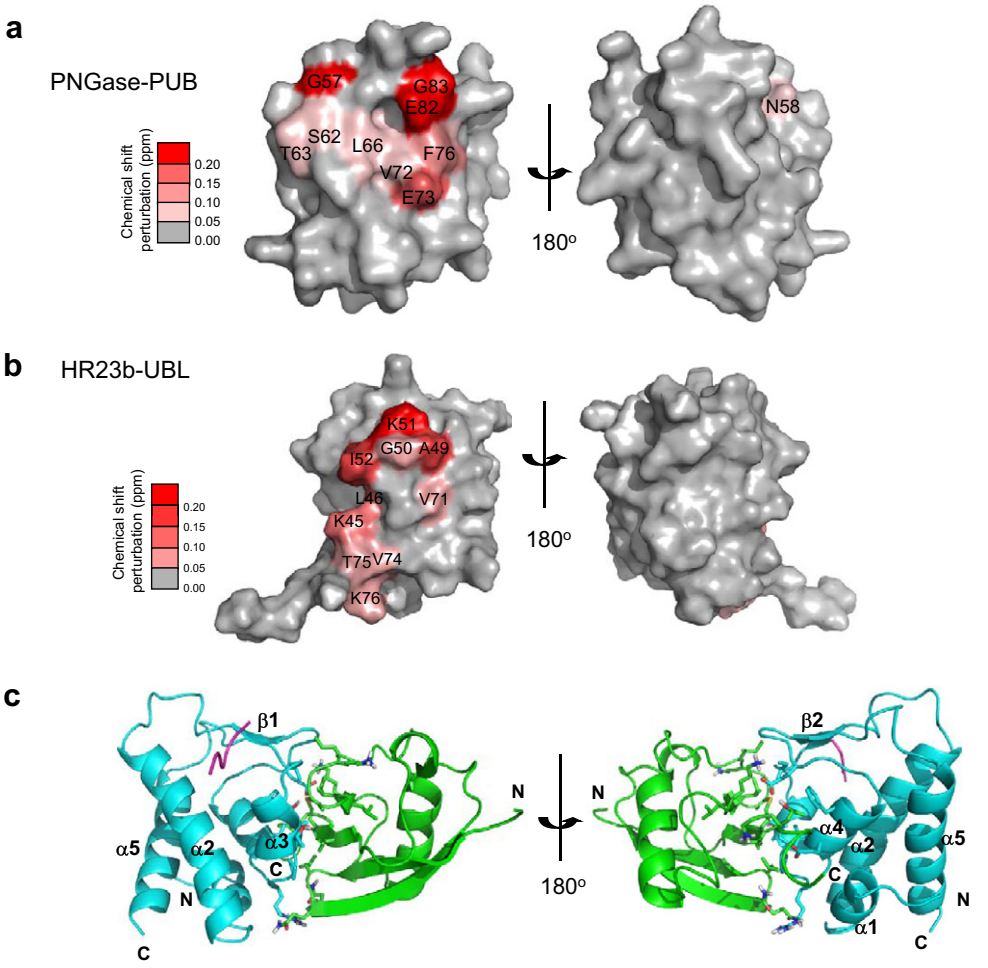

Fig. 2. NMR identification of the mode of interaction between PNGase–PUB and HR23–UBL. (a) CSP mapping of the PNGase–PUB surface involved in binding to HR23b–UBL. (b) CSP mapping of the HR23b–UBL surface involved in binding to PNGase–PUB. In (a) and (b), surface representation of PUB and UBL is done with amino acid residues colored red in gradation according to the degree of CSP. (c) 3D structural model of the ternary complex of HR23b–UBL (*green*), PNGase–PUB (*cyan*), and the C-terminal segment of p97 (*magenta*). The C-terminal segment of p97 is superimposed onto the UBL–PUB complex generated by HADDOCK by inspection of the crystal structure of PUB complexed with this segment [27].

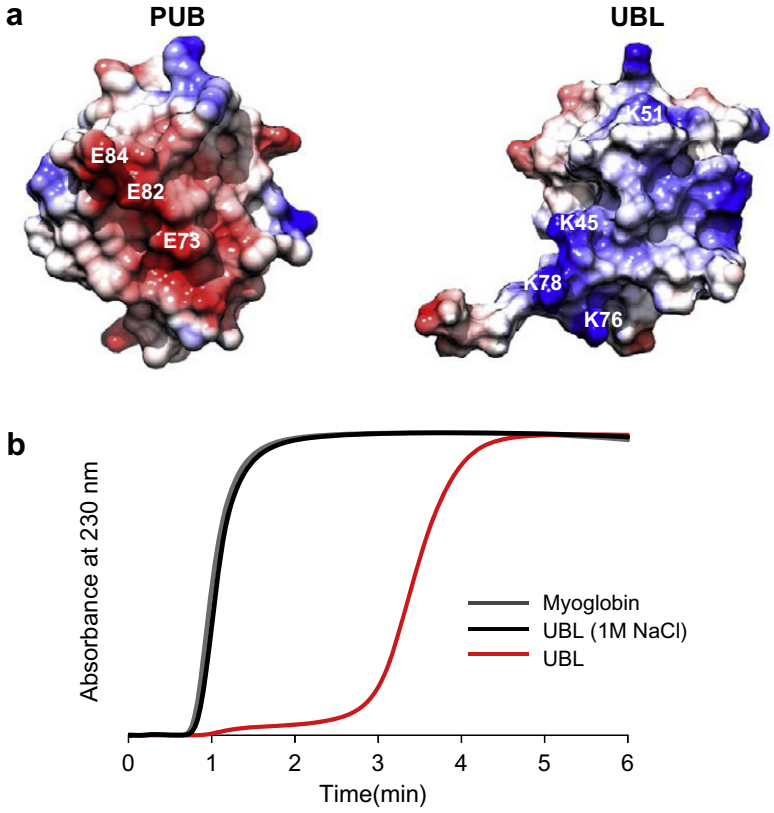

Fig. 3. Electrostatic interactions between PUB and UBL. (a) Electrostatic potential maps were overlaid on the interaction surfaces of PNGase–PUB and HR23b–UBL. (b) Effects of NaCl on the PUB–UBL interaction characterized by the FAC analyses. Elution profiles of UBL with (*black line*) or without (*red line*) 1 M NaCl are superimposed on that of the control protein, myoglobin (*gray line*).

PNGase–PUB exhibits moderately increased affinities for longer Ub chains. The association constants for HR23–UBLs were about twofold higher than that for tetra-Ub.

3.3. Interaction mode of PNGase–PUB with HR23–UBL

We also mapped the CSPs of each protein to gain insight into the binding mode of PUB and the UBL domain of HR23 (Fig. 2a and b). Supplementary Fig. 2 displays the CSP data of PNGase–PUB in the presence and absence of unlabeled HR23b–UBL. These data indicate that the PUB domain binds HR23b–UBL through its surface consisting of the α3 and α4 helices and β1–α3, α3–α4, and α4–β2 loops. The binding of Ub and HR23a–UBL also caused chemical shift changes in the almost identical set of the backbone amide resonance of PUB, although the magnitude of CSPs was lower in Ub binding (Supplementary Fig. 2).

The CSPs observed in HR23b–UBL upon binding to the PUB domain were also mapped on its 3D structure (Fig. 2b and Supplementary Fig. 3). In either case, the amino acid residues showing a CSP were localized on the hydrophobic surface widely conserved among Ub/UBLs, which is spatially close to the C-terminal segment and surrounded by basic amino acid residues.

Based on the CSP data, a 3D docking model was made for the complex formed between PNGase–PUB and HR23b–UBL using the HADDOCK program (Fig. 2c). The family of final structures had the lowest intermolecular energy (-499.78 kcal mol^{-1}) and the highest buried surface area (1853 Å^2). The average pairwise root-mean-square deviation in the best 10 structures of this cluster was 2.38 ± 1.50 Å. The binding surface of UBL is abundant in basic amino acid residues, whereas the binding surface of PUB is negatively charged, suggesting that electrostatic interactions contribute to their affinities (Fig. 3a). Indeed, the FAC analysis demonstrated that the UBL–PUB interaction was severely impaired in a high ionic strength condition (Fig. 3b).

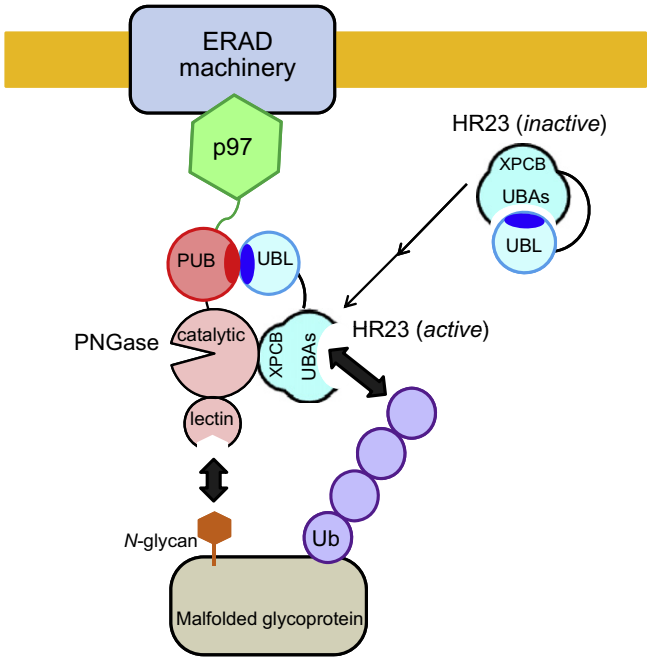

Fig. 4. A proposed mechanistic model for active complex formation between PNGase and HR23 in the ERAD machinery through the PUB–UBL interaction.

4. Discussion

To elucidate the functional roles of PUB from a structural viewpoint, we herein focused on the interaction between the UBL domain of HR23 and the PUB domain of PNGase; PNGase is one of the most extensively studied PUB-possessing proteins. We demonstrated that PNGase–PUB directly binds to the Ub domain primarily through its negatively charged surface, which electrostatically interacts with the basic amino acid residues surrounding the well-conserved hydrophobic patch of the UBL domain. This binding surface on HR23–UBL is also involved in interactions with various Ub/UBL-binding motifs, such as the Ub-interacting motif (UIM) and the coupling of Ub to ERAD (CUE) domain, as well as the UBA domain. The amino acid residues of the binding interface of mouse PNGase–PUB identified in the present study are highly conserved across mammalian species, suggesting a common ability of the PNGases to interact with Ub/UBLs through their PUB domain in competition with other Ub/UBL-binding motifs in the Ub–proteasome system. Those amino acids are well conserved in HOIP-PUB but not in Ubxd-1-PUB, suggesting some variations of their binding partners.

Our findings strongly imply that the PUB domain of PNGase contributes to the interaction with HR23, although the interaction between these two proteins have so far been assumed to be mediated between the catalytic domain of PNGase and XPCB domain of HR23 [19,45]. The crystal structure revealed that the C-terminal segment of p97 is accommodated in the positively charged groove on the surface of PNGase–PUB formed by α2–α4 and β1 [27]. The 3D model indicated no overlap between the UBL-binding interface and p97-binding site on the PUB domain, suggesting the formation of the ternary complex of PUB with p97 and simultaneously with HR23–UBL (Fig. 2c).

The PUB-binding surface of HR23–UBL is also employed for interacting with a variety of Ub/UBL-binding motifs, including the UIM of the proteasome S5a subunit and the UBA domain belonging to the same HR23 molecule [46]. This raises the intriguing possibility that PNGase–PUB and HR23–UBA compete to interact with HR23–UBL in the complex. It has been reported that the range for K_a values of the UBA–UBL interaction is $0.4–0.6 \times 10^3\ M^{-1}$ [35], which is ten times smaller (Table 1) than that of the PUB–UBL interaction, suggesting that HR23–UBL is mainly involved in the intermolecular interaction with PNGase–PUB in the complex.

HR23–UBA serves as an acceptor for Lys48-linked Ub chains with varying affinities depending on their chain lengths. Namely, both HR23–UBA and PNGase–PUB preferentially bind longer Ub chains. K_a values for monomeric Ub were $1.2 \times 10^3\ M^{-1}$ for PUB (Table 1) and $3.3 \times 10^3\ M^{-1}$ for the UBA domain [35]. The binding affinity of the UBA domain for tetra-Ub was more than ten-fold higher than that for monomeric Ub [35,47], while the affinity enhancement for PUB was only twofold. Thus, the dependency of the affinity on Ub chain length was more prominent in HR23–UBA than in PNGase–PUB.

On the basis of all these data, we propose the following working model for the functional interplay between PNGase and HR23 (Fig. 4). In the resting state, the proteasome shuttle factor HR23 exhibits a closed, inactive form in which its UBL and UBA domains intramolecularly interact with each other. Upon recruitment of HR23 to the ERAD system, the UBL domain switches to interact with PNGase–PUB, rendering the UBA domain in an open, active state for accepting an elongated Ub chain attached to the glycoprotein as an ERAD substrate, while the C-terminal lectin domain of PNGase captures the *N*-glycan for chopping by the catalytic domain.

The present data thus offer a structural basis of the ERAD function of PUB as a previously uncharacterized Ub/UBL-binding motif. Our findings imply that PNGase–PUB acts not only as a p97-binding module but also as a possible activator of HR23 in the ERAD complex, exemplifying the versatile functions of PUB in the Ub–proteasome system.

Acknowledgments

We thank Yukiko Isono (IMS) for her help in the preparation of the proteins. This work was supported, in part, by Grants in Aid for Scientific Research (18390016, 20059030, 20107004, 21370050, 21870052, and 22020039), the Targeted Proteins Research Program from the Ministry of Education, Culture, Sports, Science and Technology of Japan, and the CREST project from the Japan Science and Technology Agency.

Appendix A. Supplementary data

Supplementary data associated with this article can be found, in the online version, at http://dx.doi.org/10.1016/j.febslet.2012.03.027.

References

[1] Clague, M.J. and Urbé, S. (2010) Ubiquitin: same molecule, different degradation pathways. Cell 143, 682–685.
[2] Vucic, D., Dixit, V.M. and Wertz, I.E. (2011) Ubiquitylation in apoptosis: a post-translational modification at the edge of life and death. Nat. Rev. Mol. Cell Biol. 12, 439–452.
[3] Ligeon, L.A., Temime-Smaali, N. and Lafont, F. (2011) Ubiquitylation and autophagy in the control of bacterial infections and related inflammatory responses. Cell. Microbiol. 13, 1303–1311.
[4] Hegde, A.N. and Upadhya, S.C. (2011) Role of ubiquitin–proteasome-mediated proteolysis in nervous system disease. Biochim. Biophys. Acta 1809, 128–140.
[5] Kato, K. and Kamiya, Y. (2007) Structural views of glycoprotein-fate determination in cells. Glycobiology 17, 1031–1044.
[6] Aebi, M., Bernasconi, R., Clerc, S. and Molinari, M. (2010) *N*-glycan structures: recognition and processing in the ER. Trends Biochem. Sci. 35, 74–82.
[7] Kamiya, Y., Satoh, T., Kato, K. (2012). Molecular and structural basis for *N*-glycan-dependent determination of glycoprotein fates in cells Biochemica et Biophysica Acta-General Subjects, in press. http://dx.doi.org/10.1016/j.bbagen.2011.12.17.
[8] Smith, M.H., Ploegh, H.L. and Weissman, J.S. (2011) Road to ruin: targeting proteins for degradation in the endoplasmic reticulum. Science 334, 1086–1090.
[9] Wolf, D.H. and Stolz, A. (2012) The Cdc48 machine in endoplasmic reticulum associated protein degradation. Biochim. Biophys. Acta 1823, 117–124.
[10] Mayor, T. (2012) Navigating the ERAD interaction network. Nat. Cell Biol. 14, 46–47.
[11] Park, H., Suzuki, T. and Lennarz, W.J. (2001) Identification of proteins that interact with mammalian peptide:*N*-glycanase and implicate this hydrolase in the proteasome-dependent pathway for protein degradation. Proc. Natl. Acad. Sci. USA 98, 11163–11168.
[12] Jarosch, E., Taxis, C., Volkwein, C., Bordallo, J., Finley, D., Wolf, D.H. and Sommer, T. (2002) Protein dislocation from the ER requires polyubiquitination and the AAA-ATPase Cdc48. Nat. Cell Biol. 4, 134–139.
[13] Wiertz, E.J., Tortorella, D., Bogyo, M., Yu, J., Mothes, W., Jones, T.R., Rapoport, T.A. and Ploegh, H.L. (1996) Sec61-mediated transfer of a membrane protein from the endoplasmic reticulum to the proteasome for destruction. Nature 384, 432–438.
[14] Suzuki, T., Park, H., Hollingsworth, N.M., Sternglanz, R. and Lennarz, W.J. (2000) PNG1, a yeast gene encoding a highly conserved peptide:*N*-glycanase. J. Cell Biol. 149, 1039–1052.
[15] Chapman, E., Fry, A.N. and Kang, M. (2011) The complexities of p97 function in health and disease. Mol. BioSyst. 7, 700–710.
[16] Hirsch, C., Blom, D. and Ploegh, H.L. (2003) A role for *N*-glycanase in the cytosolic turnover of glycoproteins. EMBO J. 22, 1036–1046.
[17] Li, G., Zhao, G., Zhou, X., Schindelin, H. and Lennarz, W.J. (2006) The AAA ATPase p97 links peptide *N*-glycanase to the endoplasmic reticulum-associated E3 ligase autocrine motility factor receptor. Proc. Natl. Acad. Sci. USA 103, 8348–8353.
[18] Suzuki, T., Park, H., Kwofie, M.A. and Lennarz, W.J. (2001) Rad23 provides a link between the Png1 deglycosylating enzyme and the 26 S proteasome in yeast. J. Biol. Chem. 276, 21601–21607.
[19] Zhao, G., Zhou, X., Wang, L., Li, G., Kisker, C., Lennarz, W.J. and Schindelin, H. (2006) Structure of the mouse peptide *N*-glycanase-HR23 complex suggests co-evolution of the endoplasmic reticulum-associated degradation and DNA repair pathways. J. Biol. Chem. 281, 13751–13761.
[20] Suzuki, T., Park, H. and Lennarz, W.J. (2002) Cytoplasmic peptide:*N*-glycanase (PNGase) in eukaryotic cells: occurrence, primary structure, and potential functions. FASEB J. 16, 635–641.

[21] Zhou, X., Zhao, G., Truglio, J.J., Wang, L., Li, G., Lennarz, W.J. and Schindelin, H. (2006) Structural and biochemical studies of the C-terminal domain of mouse peptide-*N*-glycanase identify it as a mannose-binding module. Proc. Natl. Acad. Sci. USA 103, 17214–17219.
[22] Suzuki, T., Park, H., Till, E.A. and Lennarz, W.J. (2001) The PUB domain: a putative protein–protein interaction domain implicated in the ubiquitin–proteasome pathway. Biochem. Biophys. Res. Commun. 287, 1083–1087.
[23] Buchberger, A., Howard, M.J., Proctor, M. and Bycroft, M. (2001) The UBX domain: a widespread ubiquitin-like module. J. Mol. Biol. 307, 17–24.
[24] Dreveny, I. et al. (2004) p97 and close encounters of every kind: a brief review. Biochem. Soc. Trans. 32, 715–720.
[25] Allen, M.D., Buchberger, A. and Bycroft, M. (2006) The PUB domain functions as a p97 binding module in human peptide *N*-glycanase. J. Biol. Chem. 281, 25502–25508.
[26] Madsen, L., Seeger, M., Semple, C.A. and Hartmann-Petersen, R. (2009) New ATPase regulators-p97 goes to the PUB. Int. J. Biochem. Cell Biol. 41, 2380–2388.
[27] Zhao, G., Zhou, X., Wang, L., Li, G., Schindelin, H. and Lennarz, W.J. (2007) Studies on peptide:*N*-glycanase-p97 interaction suggest that p97 phosphorylation modulates endoplasmic reticulum-associated degradation. Proc. Natl. Acad. Sci. USA 104, 8785–8790.
[28] Madsen, L., Andersen, K.M., Prag, S., Moos, T., Semple, C.A., Seeger, M. and Hartmann-Petersen, R. (2008) Ubxd1 is a novel co-factor of the human p97 ATPase. Int. J. Biochem. Cell Biol. 40, 2927–2942.
[29] Li, G., Zhao, G., Schindelin, H. and Lennarz, W.J. (2008) Tyrosine phosphorylation of ATPase p97 regulates its activity during ERAD. Biochem. Biophys. Res. Commun. 375, 247–251.
[30] Doerks, T., Copley, R.R., Schultz, J., Ponting, C.P. and Bork, P. (2002) Systematic identification of novel protein domain families associated with nuclear functions. Genome Res. 12, 47–56.
[31] Walters, K.J., Lech, P.J., Goh, A.M., Wang, Q. and Howley, P.M. (2003) DNA-repair protein hHR23a alters its protein structure upon binding proteasomal subunit S5a. Proc. Natl. Acad. Sci. USA 100, 12694–12699.
[32] Hirano, T., Serve, O., Yagi-Utsumi, M., Takemoto, E., Hiromoto, T., Satoh, T., Mizushima, T. and Kato, K. (2011) Conformational dynamics of wild-type Lys-48-linked diubiquitin in solution. J. Biol. Chem. 286, 37496–37502.
[33] Yagi-Utsumi, M., Matsuo, K., Yanagisawa, K., Gekko, K., Kato, K. (2011). Spectroscopic characterization of intermolecular interaction of amyloid β promoted on GM1 micelles. Int. J. Alzheimer's Dis. 2011, Article ID 925073, p. 8.
[34] Satoh, T., Sakata, E., Yamamoto, S., Yamaguchi, Y., Sumiyoshi, A., Wakatsuki, S. and Kato, K. (2010) Crystal structure of cyclic Lys48-linked tetraubiquitin. Biochem. Biophys. Res. Commun. 400, 329–333.
[35] Ryu, K.S., Lee, K.J., Bae, S.H., Kim, B.K., Kim, K.A. and Choi, B.S. (2003) Binding surface mapping of intra- and interdomain interactions among hHR23B, ubiquitin, and polyubiquitin binding site 2 of S5a. J. Biol. Chem. 278, 36621–36627.
[36] Varadan, R., Assfalg, M., Haririnia, A., Raasi, S., Pickart, C. and Fushman, D. (2004) Solution conformation of Lys63-linked di-ubiquitin chain provides clues to functional diversity of polyubiquitin signaling. J. Biol. Chem. 279, 7055–7063.
[37] Delaglio, F., Grzesiek, S., Vuister, G.W., Zhu, G., Pfeifer, J. and Bax, A. (1995) NMRPipe: a multidimensional spectral processing system based on UNIX pipes. J. Biomol. NMR 6, 277–293.
[38] Goddard, T.D. and Koeller, D.G. (1993) Sparky, University of California, San Francisco, CA.
[39] Kasai, K., Oda, Y., Nishikawa, M. and Ishii, S. (1986) Frontal affinity chromatography: theory for its application to studies on specific interactions of biomolecules. J. Chromatogr. 376, 33–47.
[40] Kamiya, Y. et al. (2005) Sugar-binding properties of VIP36, an intracellular animal lectin operating as a cargo receptor. J. Biol. Chem. 280, 37178–37182.
[41] Kamiya, Y., Kamiya, D., Yamamoto, K., Nyfeler, B., Hauri, H.P. and Kato, K. (2008) Molecular basis of sugar recognition by the human L-type lectins ERGIC-53, VIPL, and VIP36. J. Biol. Chem. 283, 1857–1861.
[42] Dominguez, C., Boelens, R. and Bonvin, A.M. (2003) HADDOCK: a protein–protein docking approach based on biochemical or biophysical information. J. Am. Chem. Soc. 125, 1731–1737.
[43] de Vries, S.J., van Dijk, A.D., Krzeminski, M., van Dijk, M., Thureau, A., Hsu, V., Wassenaar, T. and Bonvin, A.M. (2007) HADDOCK versus HADDOCK: new features and performance of HADDOCK2.0 on the CAPRI targets. Proteins 69, 726–733.
[44] Brünger, A.T. et al. (1998) Crystallography & NMR system: a new software suite for macromolecular structure determination. Acta Crystallogr. D Biol. Crystallogr. 54, 905–921.
[45] Li, G., Zhou, X., Zhao, G., Schindelin, H. and Lennarz, W.J. (2005) Multiple modes of interaction of the deglycosylation enzyme, mouse peptide *N*-glycanase, with the proteasome. Proc. Natl. Acad. Sci. USA 102, 15809–15814.
[46] Winget, J.M. and Mayor, T. (2010) The diversity of ubiquitin recognition: hot spots and varied specificity. Mol. Cell 38, 627–635.
[47] Raasi, S., Orlov, I., Fleming, K.G. and Pickart, C.M. (2004) Binding of polyubiquitin chains to ubiquitin-associated (UBA) domains of HHR23A. J. Mol. Biol. 341, 1367–1379.